

DOI: 10.13957/j.cnki.tcx.2023.02.007

Cordierite-based Ceramics with Low Thermal Expansion Coefficient from Clay and Coal Fly Ash

CHENG Ling¹, XIAO Zhuohao¹, XIAO Xiaodong¹, LI Xiuying¹,
DONG Hongbo², KONG Lingbing¹

(1. Jingdezhen Ceramic University, Jingdezhen 333403, Jiangxi, China;

2. Linyi University, Linyi 276005, Shandong, China)

Abstract: Low-cost synthesis of cordierite ceramic materials has been widely concerned. In this study, clay, fly ash, talc and bauxite were used as the main raw materials to prepare low-expansion cordierite ceramics. The effects of composition of the raw materials and sintering condition on structural characteristics of the ceramics, such as phase content, micromorphology, thermal expansion coefficient, porosity and so on, were systematically studied. It is found that the content of talc had a significant effect on phase composition of the cordierite ceramics. When the content of talc was 33.14 wt.%, single phase cordierite ceramics can be obtained. Excessive talc would lead to the formation of spinel olivine phase. The increase in sintering temperature and time is helpful for the phase formation of cordierite. After sintering at 1300 °C for 3.5 h, the cordierite ceramics had a minimum thermal expansion coefficient of $2.21 \times 10^{-6} \text{ }^{\circ}\text{C}^{-1}$ and a strength of 36.17 MPa.

Key words: low-cost; cordierite; thermal expansion coefficient

1 Introduction

Cordierite ($2\text{MgO} \cdot 2\text{Al}_2\text{O}_3 \cdot 5\text{SiO}_2$) is magnesium aluminum silicate, as a product of thermal metamorphism of clays in nature. It belongs to orthorhombic crystalline system, with pseudohexagonal structure, density of $2.53 \text{ g} \cdot \text{cm}^{-3}$ and melting point of 1470 °C^[1-2]. Cordierite based ceramics have unique properties, such as low coefficient of thermal expansion, low dielectric constant, high thermal shock resistance, high chemical stability and strong mechanical strength^[3]. Therefore, they have been widely used in the fields of refractory, electrical insulators, porous ceramic membranes, integrated circuit boards and so on^[4]. However, because cordierite is a less abundant mineral in nature and its purity is not sufficiently high, it cannot meet the requirement of industrial applications. Therefore, it is necessary to synthesize cordierite and cordierite based ceramic materials, by using different starting materials and processing techniques.

Due to the cost-effectiveness, solid-state reaction methods with naturally abundant raw materials are still the most attractive in synthesis of cordierite based ceramic materials. Ren et al. prepared cordierite with Suzhou clay, talc and

industrial alumina as the main raw materials by using solid-state sintering reaction method at about 1350 °C. The optimal composition of the raw materials was 39.04% talc, 46.08% Suzhou clay and 14.88% industrial alumina^[5]. Redaoui et al. explored the possibility to synthesize low-cost cordierite ceramic materials with Algerian kaolinite combined with magnesium oxide, where crystallization kinetics mechanism was studied. As a result, high-density cordierite ceramics were obtained at 1250 °C^[6]. Harati et al. developed cordierite ceramic materials with desirable chemical properties and thermal stability, with low-cost natural Moroccan kaolin and peridotite as the main raw materials^[7].

Due to the nonrenewable nature of mineral resources and the increasing demand for ceramic products, the synthesis of cordierite from solid wastes has drawn significant attention. As an attractive solid waste, fly ash is mostly amorphous in most cases^[8]. Because the main components of fly ash are Al_2O_3 and SiO_2 , which can be used as promising sources for the preparation of cordierite and other ceramic materials^[9], it has been fully studied in the field of cordierite based ceramic materials^[10]. Ma et al. examined the effect of composition of raw materials on microstructure of

Received date: 2023-01-06.

Revised date: 2023-03-17.

Funding Information: National Natural Science Foundation of China (51962013 and 52172070), Key R&D Program of Jiangxi Province (jxsq2019201036, 20223AAE02010 and 20201BBE51011), Key Projects of Jingdezhen Science and Technology Bureau (2021ZDGG006).

Correspondent author: XIAO Zhuohao (1978-), Male, Ph.D., Professor; Dong Hongbo (1972-), Male, Ph.D., Professor.

E-mail: xiaozhuohao@126.com; donghbo@163.com

the products from high alumina fly ash, industrial sintered MgO and SiO₂ powders^[11]. It was found that the sample synthesized at 1280 °C had large content of α -cordierite and β -cordierite, with MgO-rich compositions to be optimal. Kumar et al. produced phase pure cordierite and cordierite ceramics doped with ZrO₂, CeO₂ and TiO₂, from fly ash waste, while studying mechanical properties of the cordierite ceramics, such as hardness, fracture toughness and flexural strength^[12]. The cordierite-ZrO₂ (5–20 wt.%) sample exhibited the highest hardness and flexural strength, with a Vickers hardness of 7.04 GPa, a fracture toughness of 3.47 MPa·m^{1/2} and a flexural strength of 196.72 MPa. Cordierite synthesized in this way can be used as catalyst substrate material with suitable mechanical properties.

In this work, we report the synthesis of cordierite by using clay and fly ash as the main raw materials, together with talc and bauxite, in order to reduce the cost of cordierite based ceramic materials. The effects of sintering condition and content of talc on phase composition and properties of the cordierite ceramic samples were studied, in order to explore reasonable process parameters to prepare cordierite ceramic materials with desired thermal properties and hence promote the production and application of low-cost cordierite ceramics.

2 Experimental

2.1 Sample preparation

Cordierite based ceramics were prepared by solid-state reaction method, with clay and fly ash as

the main raw materials, together with talc and bauxite as additives. Chemical compositions of all the raw materials were characterized by using XRF, as listed in Tab. 1. Based on the chemical composition analysis results, the clay and fly ash could be used to the maximized degree, with talc as the source of MgO, sample M1 was designed according to the stoichiometric composition of cordierite. Noting the effect of MgO reported in the open literature^[13–14], M series samples were designed as listed in Tab. 2, in order to study the effect of MgO.

Raw materials were mixed thoroughly according to the compositions in Tab. 2. The mixtures were pressed into cuboid samples with mass of 4 g and dimension of 40 mm×10 mm×5 mm. After drying in an oven at 100–105 °C for 2 h, the cuboid samples were sintered at 1200 °C, 1250 °C, 1275 °C, 1300 °C and 1325 °C for 0.5 h, at a heating rate of 10 °C·min⁻¹.

2.2 Characterization

Coefficient of the samples was measured by using a dilatometer (PCY-III-1400) up to 600 °C, at a heating rate of 5 °C·min⁻¹. A computerized electronic universal testing machine (WDW-20) was used to measure flexural strength of the samples, at a loading rate of 0.1 mm·s⁻¹. Density and porosity of the samples were examined according to the Archimedes principle, with distilled water as the soaking medium. Phase composition was characterized by using Bruker D/MAX 2500 type X-ray diffractometer, over 5°–70°, at a step of 0.02°. Microstructure of the ceramic samples was observed by using Hitachi SU-8010 type scanning electron microscopy.

Tab. 1 Chemical compositions of the raw materials (wt.%)

Ingredients	SiO ₂	Al ₂ O ₃	CaO	MgO	K ₂ O	Na ₂ O	TiO ₂	Fe ₂ O ₃	I.L.
Clay	65.50	16.84	0.35	1.23	2.37	0.54	0.90	5.34	6.64
Fly ash	43.06	21.57	1.72	0.85	1.29	0.42	0.84	3.44	26.28
Bauxite	23.76	70.69	—	0.34	—	0.20	2.79	0.96	1.26
Talc	60.95	1.07	0.32	30.81	0.01	0.01	0.05	1.27	5.49

Tab. 2 Raw material compositions of the samples (wt.%)

No.	Raw material composition					MgO	Impurity
	Clay	Fly ash	Bauxite	Talc	Total		
M1	14.74	21.06	31.06	33.14	100.00	11.26	5.30
M2	11.44	16.34	33.12	39.10	100.00	13.11	4.68
M3	8.13	11.61	35.20	45.06	100.00	15.00	4.09
M4	4.84	6.92	37.26	50.98	100.00	16.66	3.51
M5	1.57	2.24	39.31	56.88	100.00	18.35	2.95

3 Results and Discussion

3.1 Effect of raw materials composition on phase formation

Fig. 1 shows XRD patterns of M1, M3 and M5, which were sintered at 1200 °C for 0.5 h. The presence of talc has a strong effect on phase composition of the samples. For M1 with stoichiometric composition of cordierite, cordierite and indialite are present as the major crystalline phases. For M3 and M5, ringwoodite $[(\text{Mg}, \text{Fe})_2\text{SiO}_4]$, periclase (MgO) and quartz (SiO_2) are additionally observed, as minor phases. This is because Fe^{2+} was involved in the crystallization process, replacing Mg^{2+} in the cordierite crystalline structure to form spinel olivine. The diffraction peaks of cordierite in M3 were strengthened as compared with those in M1. This is probably because the content of clay and fly ash containing low melting point components (K_2O , Na_2O) was decreased, due to the addition of talc, leading to reduction in the content of low melting point glass phase^[15]. As a result, since the erosion of the cordierite became less serious, the weakening in the diffraction peaks of cordierite in M5 is attributed to the stoichiometric deviation.

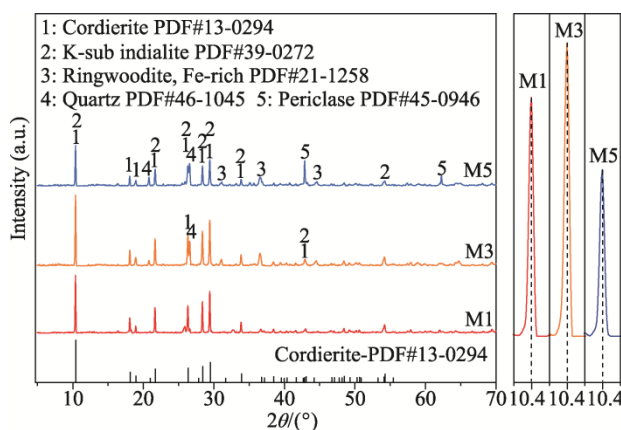


Fig. 1 XRD patterns of representative samples sintered at 1200 °C for 0.5 h

Fig. 2 shows XRD patterns of M1, M3 and M5 sintered at 1275 °C for 0.5 h. As the sintering temperature was increased, the secondary phase periclase and quartz disappeared, while the spinel peridotite was transferred to magnesium peridotite. The peak intensity of cordierite was gradually decreased with increasing content of talc, with that in sample M1 to be the strongest. With excessive MgO , the effect of K_2O and Na_2O was suppressed by that of MgO . Due to the formation

of forsterite, the content of crystalline cordierite was decreased^[16–17].

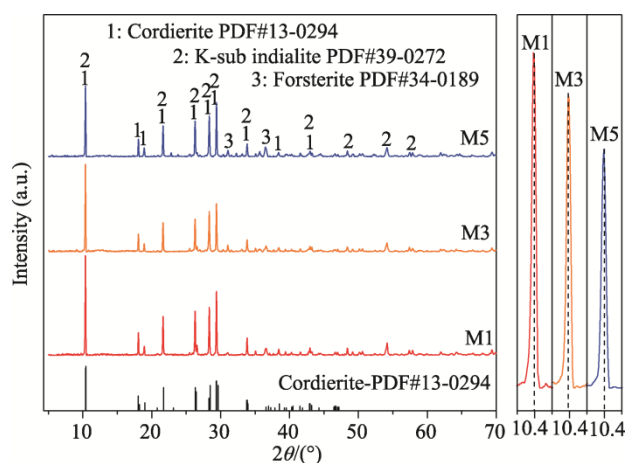


Fig. 2 XRD patterns of representative samples sintered at 1275 °C for 0.5 h

3.2 Effect of sintering temperature on microstructure and properties

XRD patterns of M1 sintered at different temperatures for 0.5 h are depicted in Fig. 3 (a), while SEM image of this sample sintered at 1300 °C for 0.5 h is shown in Fig. 3 (b). After sintering at different temperatures, the major phases in M1 are cordierite and indialite. With increasing sintering temperature, the peak intensity of cordierite is gradually increased, suggesting that high sintering temperature is beneficial to the crystallization of cordierite. In addition, cordierite peaks are observed in the sample after sintering at 1200 °C, which is lower than the cordierite phase formation temperature reported previously^[18]. The reduction in cordierite phase formation temperature is readily ascribed to the presence of alkali and alkaline earth metal oxides, such as CaO , Na_2O , K_2O and so on, which offered liquid phase to promote the crystallization of cordierite in the samples^[19]. The cordierite phase is present as granular or needle-shaped irregular crystals, which are separated by glass phase, implying that sintering time is not sufficiently long to ensure the growth of cordierite^[20].

Cordierite has coefficient of thermal expansion (CTE) in the range of 1.0×10^{-6} – 5.0×10^{-6} °C⁻¹, depending on phase composition and content in the ceramics^[21–22]. Fig. 4 shows CTE values of the samples as a function of sintering temperature. No CTE data are available for the samples molten in the sintering process^[23]. With increasing sintering temperature, CTE values of the samples tended to decrease, owing to the crystallization of cordierite from the matrix. This observation is in a good agreement with the XRD results.

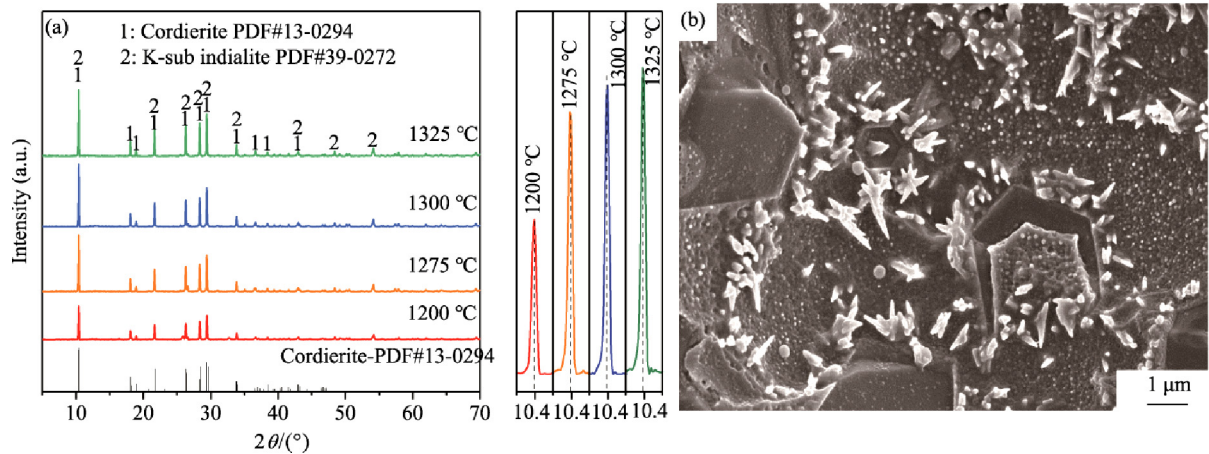


Fig. 3 (a) XRD patterns of M1 sintered at different temperatures. (b) SEM image of M1 sintered at 1300 °C for 0.5 h

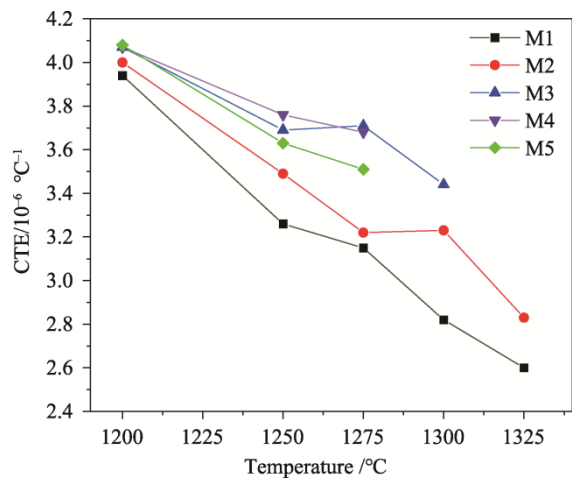


Fig. 4 Coefficient of thermal expansion of the samples as a function of sintering temperature

Density and porosity of the samples sintered at different temperatures for 0.5 h are listed in Tab. 3 and Tab. 4. With increasing sintering temperature, density is gradually increased and the porosity is decreased, because the densification process of the samples was promoted by the crystallization of cordierite [24]. At a given sintering temperature, the sample density is increased with increasing content of MgO, while porosity is also increased. On one hand, excessive MgO hindered the crystallization of cordierite ($2.53 \text{ g}\cdot\text{cm}^{-3}$), while forsterite with higher density ($3.33 \text{ g}\cdot\text{cm}^{-3}$) was formed instead, resulting in increase in sample density [25]. On the other hand, with increasing content of talc, the level of impurity in the samples was decreased, so that the content of liquid phase is reduced. As a consequence, the pores could not be fully filled, i.e., porosity was increased [26].

Flexural strength is an important mechanical property of low expansion ceramics, which is dependent on phase composition, crystal size, size distribution and so on [27]. Flexural strengths of the samples sintered at different temperatures are listed in Tab. 5, with

increasing sintering temperature, the flexural strength is gradually increased, which is consistent with the variation trend in density, owing to the crystallization of cordierite and increment in the content of glass phase. At a given sintering temperature, the flexural strength is decreased with increasing content of talc, which follows the trend in porosity.

Tab. 3 Density of the samples sintered at different temperatures ($\text{g}\cdot\text{cm}^{-3}$)

No.	1200 °C	1250 °C	1275 °C	1300 °C	1325 °C
M1	1.97	2.07	2.09	2.18	2.06
M2	2.10	2.15	2.17	2.21	2.03
M3	2.12	2.13	2.34	2.23	—
M4	2.21	2.28	2.35	—	—
M5	2.21	2.26	2.36	—	—

Tab. 4 Porosity of the samples sintered at different temperatures (%)

No.	1200 °C	1250 °C	1275 °C	1300 °C	1325 °C
M1	34.50	30.76	27.33	27.93	22.82
M2	33.18	34.24	29.89	29.16	22.52
M3	35.08	36.54	30.62	22.08	—
M4	37.46	36.32	31.25	—	—
M5	39.91	36.88	29.84	—	—

Tab. 5 Flexural strength of the samples sintered at different temperatures (MPa)

No.	1200 °C	1250 °C	1275 °C	1300 °C	1325 °C
M1	24.0	21.5	27.0	26.5	25.5
M2	21.5	21.5	26.5	25.5	31.5
M3	17.0	23.0	21.5	30.0	—
M4	13.0	16.5	20.5	—	—
M5	10.0	18.0	23.0	—	—

3.3 Effect of sintering time on microstructure and properties

Since M1 sintered at 1300 °C has the highest performance, it was used to study the effect of sintering time. XRD patterns of M1 sintered at 1300 °C for 0.5 h and 3.5 h are shown in Fig. 5 (a). Cross-sectional SEM image of M1 sintered at 1300 °C for 3.5 h is illustrated in Fig. 5 (b). With increasing sintering time, the peak intensity of cordierite is gradually increased, implying the continuous crystallization of cordierite. The cordierite crystals are hexagonal prismatic in shape, with different grain sizes and interlocking behavior. Therefore, prolonging sintering time is beneficial to the crystallization and growth of cordierite phase. With increasing crystal size of cordierite, density of the samples is increased and the porosity is decreased.

Microstructural and mechanical properties of M1 samples sintered at 1300 °C for different times are depicted in Fig. 6. As seen in Fig. 6 (a), with increasing sintering time, the porosity increases slightly until 2.5 h and then decreases. Meanwhile,

density of the samples monotonically increased with sintering time. CTE value is decreased with increasing sintering time, which is consistent with the variation trend in XRD peak intensity of cordierite, as observed in Fig. 6 (b). Flexural strength of ceramics is dependent on their microstructure and porosity. In the sintering time of 0.5-2.5 h, although the porosity increases, the flexural strength is rising. After sintering for 2.5 h, flexural strength of the sample started to decrease, due to the increase in porosity. However, as the sintering time was increased to 3.5 h, because the porosity is significantly reduced, the flexural strength is largely increased. The simultaneous increase in porosity and flexural strength could ascribed to the fact that the content of the liquid phase generated due to the presence of impurities and oxides in the raw materials is not sufficiently high to completely fill the pores in the samples, but the prolongation of the sintering time promoted the crystallization and growth of cordierite, resulting in overall increase in porosity and flexural strength^[28].

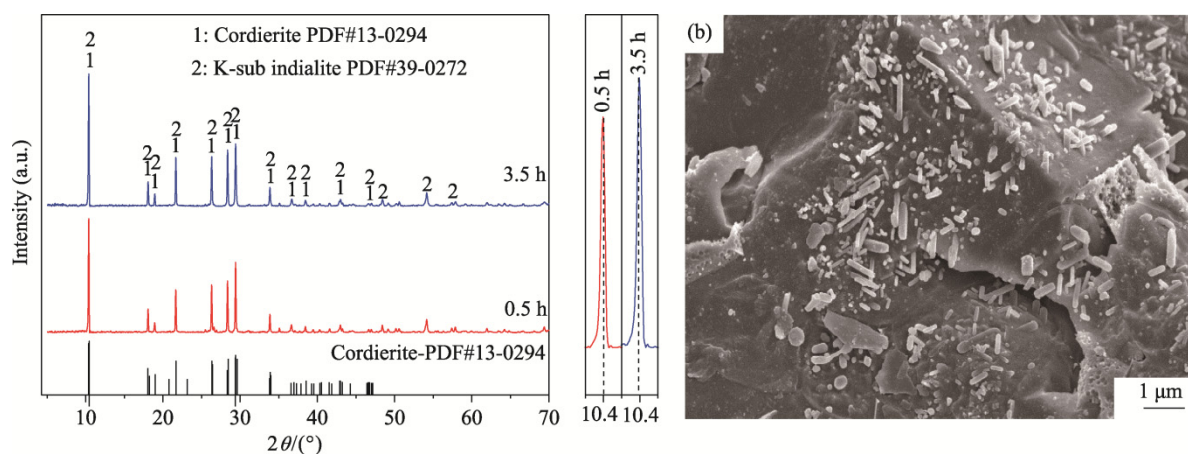


Fig. 5 (a) XRD patterns of M1 sintered at 1300 °C for different times. (b) SEM image of M1 sintered at 1300 °C for 3.5 h

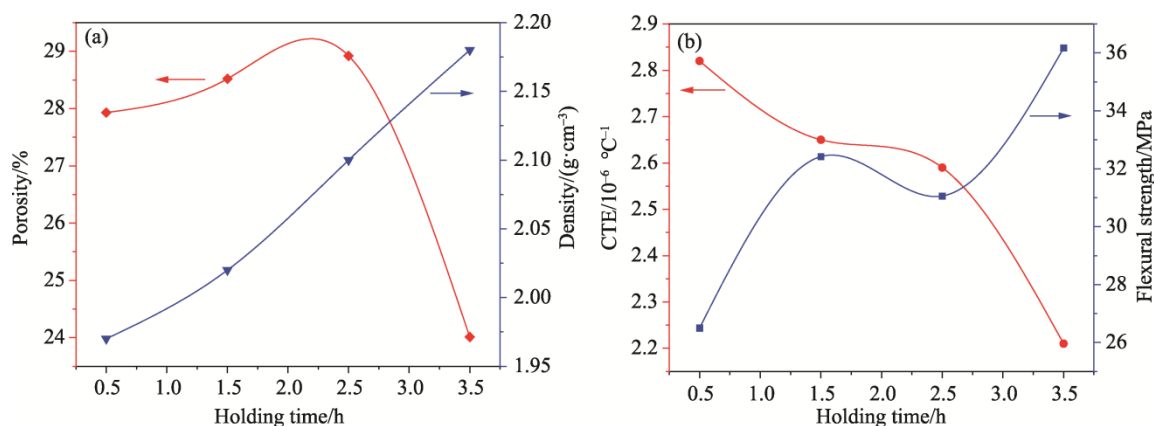


Fig. 6 Structural and mechanical properties of M1 samples sintered at 1300 °C as a function of sintering time: (a) porosity and density and (b) thermal expansion coefficient and flexural strength

4 Conclusions

Cordierite based low thermal expansion ceramics could be developed by using solid-state reaction method, with fly ash, clay, bauxite and talc as main raw materials. The addition of talc has a significant effect on microstructure and properties of the cordierite ceramics. Excessive content of talc promoted the formation of forsterite, leading to increase in the coefficient of thermal expansion (CTE) of the samples. The cordierite sample with 33.14 wt.% talc sintered at 1300 °C had CTE value of $2.82 \times 10^{-6} \text{ }^{\circ}\text{C}^{-1}$ and flexural strength of 26.5 MPa.

Sintering time also had effect on microstructure and properties of the cordierite ceramics to a certain degree. Appropriate prolonging the sintering time is beneficial to promote densification, reduce coefficient of thermal expansion of the material and improve mechanical properties of the cordierite ceramics. The M1 sample sintered at 1300 °C for 3.5 h exhibited CTE value of $2.21 \times 10^{-6} \text{ }^{\circ}\text{C}^{-1}$ and flexural strength of 36.17 MPa.

References:

- [1] OROSCO P, RUIZ M D C, GONZÁLEZ J. Synthesis of cordierite by dolomite and kaolinitic clay chlorination. Study of the phase transformations and reaction mechanism [J]. Powder Technology, 2014, 267: 111–118.
- [2] ZHOU S J, WANG F, HE Z Y, et al. Effect of element doping on structure and properties of cordierite ceramics [J]. Journal of Ceramics, 2022, 43(2): 196–206. (in Chinese)
- [3] ZHENG L P, ZHANG S H, YAN G Y. Research progress of cordierite refractories [J]. Shandong Ceramics, 2013, 36(1): 14–18. (in Chinese)
- [4] BANJURAIZAH J, MOHAMAD H, AHMAD Z A. Crystal structure of single phase and low sintering temperature of α -cordierite synthesized from talc and kaolin [J]. Journal of Alloys and Compounds, 2009, 482(1/2): 429–436.
- [5] REN X H. Research on the preparation of cordierite with kaolin-talc-alumina [J]. Advanced Ceramics, 2013, 34(3): 11–13. (in Chinese)
- [6] REDAOUI D, SAHNOUNE F, HERAIZ M, et al. Phase formation and crystallization kinetics in cordierite ceramics prepared from laplinitite and magnesite [J]. Ceramics International, 2018, 44(4): 3649–3657.
- [7] HARRATI A, ARKAME Y, MANNI A, et al. Cordierite-based refractory ceramics from natural halloysite and peridotite: Insights on technological properties [J]. Journal of the Indian Chemical Society, 2022, 99(6): 100496.
- [8] ZUO X J, WANG C, FEI Q F, et al. Progress in preparation of inorganic ceramics by fly ash [J]. Anhui Agricultural Science Bulletin, 2017, 23(16): 89–94. (in Chinese)
- [9] PETRUS H, OLVIANAS M, SUPRAPTA W, et al. Cenospheres characterization from indonesian coal-fired power plant fly ash and their potential utilization [J]. Journal of Environmental Chemical Engineering, 2020, 8(5): 104116.
- [10] WANG S X, WANG H, CHEN Z W, et al. Fabrication and characterization of porous cordierite ceramics prepared from fly ash and natural minerals [J]. Ceramics International, 2019, 45(15): 18306–18314.
- [11] MA L J, YANG P, XUE Q H, et al. Study on the microstructures of cordierite ceramics using high-alumina fly ash [J]. Journal of Xi'an University of Architecture and Technology (Natural Science Edition), 2017, 49(1): 141–144. (in Chinese)
- [12] SENTHIL KUMAR M, VANMATHI M, SENGUTTUVAN G, et al. Fly ash constituent-silica and alumina role in the synthesis and characterization of cordierite based ceramics [J]. Silicon, 2019, 11(6): 2599–2611.
- [13] JIANG W H, YU Q X, MIAO L F, et al. Effect of different raw materials and synthesis temperature on the thermal expansion coefficient of synthetic cordierite [J]. Journal of Ceramics, 2009, 30(3): 318–321. (in Chinese)
- [14] HE Y, ZHOU H P, HUANG Z L, et al. Low-temperature combustion synthesis of cordierite powder and its properties [J]. Rare Metal Materials and Engineering, 2009, 38(S2): 63–66. (in Chinese)
- [15] WANG C, PENG T J, SUN H J, et al. Preparation and physicochemical properties of porous cordierite ceramics from asbestos tailings and fly ash [J]. Bulletin of the Chinese Ceramic Society, 2022, 42(1): 151–161. (in Chinese)
- [16] GOREN R, GOCMEZ H, OZGUR C. Synthesis of cordierite powder from talc, diatomite and alumina [J]. Ceramics International, 2006, 32(4): 407–409.
- [17] BANJURAIZAH J, MOHAMAD H, AHMAD Z A. Thermal expansion coefficient and dielectric properties of non-stoichiometric cordierite compositions with excess MgO mole ratio synthesized from mainly kaolin and talc by the glass crystallization method [J]. Journal of Alloys and Compounds, 2010, 494(1/2): 256–260.

- [18] MARIKKANNAN S K, AYYASAMY E P. Synthesis, characterisation and sintering behaviour influencing the mechanical, thermal and physical properties of cordierite-doped TiO_2 [J]. Journal of Materials Research and Technology, 2013, 2(3): 269–275.
- [19] ZARGAR H R, OPREA C, OPREA G, et al. The effect of nano- Cr_2O_3 on solid-solution assisted sintering of MgO refractories [J]. Ceramics International, 2012, 38(8): 6235–6241.
- [20] DE ALMEIDA E P, DE BRITO I P, FERREIRA H C, et al. Cordierite obtained from compositions containing kaolin waste, talc and magnesium oxide [J]. Ceramics International, 2018, 44(2): 1719–1725.
- [21] KUSCER D, BANTAN I, HROVAT M, et al. The microstructure, coefficient of thermal expansion and flexural strength of cordierite ceramics prepared from alumina with different particle sizes [J]. Journal of the European Ceramic Society, 2017, 37(2): 739–746.
- [22] WANG W B, SHI Z M, WANG X G, et al. The phase transformation and thermal expansion properties of cordierite ceramics prepared using drift sands to replace pure quartz [J]. Ceramics International, 2016, 42(3): 4477–4485.
- [23] LAO X B, XU X Y, JIANG W H, et al. Effect of excess MgO on microstructure and thermal properties of cordierite ceramics for high-temperature thermal storage [J]. Ceramics International, 2019, 45(17): 22264–22272.
- [24] SEMBIRING S, SIMANJUNTAK W, SITUMEANG R, et al. Preparation of refractory cordierite using amorphous rice husk silica for thermal insulation purposes [J]. Ceramics International, 2016, 42(7): 8431–8437.
- [25] BANJURAIZAH J, MOHAMAD H, AHMAD Z A. Effect of excess MgO mole ratio in a stoichiometric cordierite ($2\text{MgO} \cdot 2\text{Al}_2\text{O}_3 \cdot 5\text{SiO}_2$) composition on the phase transformation and crystallization behavior of magnesium aluminum silicate phases [J]. International Journal of Applied Ceramic Technology, 2011, 8(3): 637–645.
- [26] LIU C B, LIU L B, TAN K F, et al. Fabrication and characterization of porous cordierite ceramics prepared from ferrochromium slag [J]. Ceramics International, 2016, 42(1): 734–742.
- [27] DE BRITO I P, DE ALMEIDA E P, DE ARAÚJO N G, et al. Development of cordierite/mullite composites using industrial wastes [J]. International Journal of Applied Ceramic Technology, 2020, 18(1): 253–261.
- [28] LI H, LI C W, WANG C A. Preparation and characterization of porous cordierite ceramics with lightweight and high strength [J]. Journal of Ceramics, 2021, 42(4): 632–638. (in Chinese)

以黏土和粉煤灰为主要原料制备低热膨胀系数堇青石基陶瓷

程 灵¹, 肖卓豪¹, 肖晓东¹, 李秀英¹, 董洪波², 孔令兵¹

(1. 景德镇陶瓷大学, 江西 景德镇 333403; 2. 临沂大学, 山东 临沂 276005)

摘 要: 低成本合成堇青石陶瓷材料一直受到研究者的广泛关注。以黏土、粉煤灰、滑石和铝矾土为主要原料制备低膨胀堇青石质陶瓷, 研究了四种原料的配比及烧成制度对陶瓷物相、显微形貌、热膨胀系数、孔隙率的影响规律。结果表明: 滑石添加量的改变显著影响堇青石陶瓷的相组成, 当滑石添加量为 33.14 wt.% 时可以获得纯堇青石相的陶瓷, 过量滑石将导致尖晶橄榄石的生成; 烧成温度的升高和保温时间的延长有助于试样中堇青石的合成, 在 1300 °C 保温 3.5 h 的烧成条件下, 可得到热膨胀系数最低为 $2.21 \times 10^{-6} \text{ } ^\circ\text{C}^{-1}$ 、强度为 36.17 MPa 的纯相堇青石质陶瓷材料。

关键词: 低成本; 堇青石; 热膨胀系数

中图分类号: TQ174.75

文献标志码: A

文章编号: 1000-2278(2023)02-0272-07

(编辑 梁华银)